

Protamine and BSA–dextran complex emulsion improves oral bioavailability and anti-tumor efficacy of paclitaxel

Guangrui Xu, Xiaoyan Bao and Ping Yao

State Key Laboratory of Molecular Engineering of Polymers, Collaborative Innovation Center of Polymers and Polymer Composite Materials, Department of Macromolecular Science, Fudan University, Shanghai, China

ABSTRACT

Food protein and polysaccharide complex emulsions are safe carriers of hydrophobic drugs and nutrients. To improve oral bioavailability and therapeutic/healthy efficacy of hydrophobic drugs and nutrients, herein, protamine (PRO), a cationic cell-penetrating peptide, was introduced into protein and polysaccharide complex emulsion. The electrostatic complex of PRO and BSA–dextran conjugate (BD) produced by Maillard reaction was used as emulsifier to produce oil-in-water emulsion (@BD/PRO). The BSA molecules were crosslinked at the oil–water interface by a heat treatment and the PRO chains were simultaneously anchored in the interface. BD emulsion (@BD) without PRO was produced for comparison. Paclitaxel (PTX), a hydrophobic antineoplastic drug, was encapsulated in the emulsions with 99% loading efficiency and 6.4% loading capacity. The emulsions had long-term stability. The bioavailability and H22 tumor inhibition efficacy of PTX@BD/PRO were 40% and 70% higher than those of PTX@BD, respectively, after oral administration in the mice. More importantly, orally administered PTX@BD/PRO had the same anti-tumor efficacy as intravenously injected commercial PTX injection. No abnormality was observed in the main organs of the mice after consecutive oral administration of PTX@BD/PRO. This study indicates that @BD/PRO is an excellent carrier of hydrophobic drugs/nutrients and is suitable for long-term oral administration.

ARTICLE HISTORY

Received 24 August 2020
Revised 10 September 2020
Accepted 14 September 2020

KEYWORDS

BSA; dextran; protamine; paclitaxel; emulsion; hydrophobic drug; oral delivery


1. Introduction

Oral medication is the most acceptable way to achieve therapeutic and healthy efficacy, especially for long-term administration (Thanki et al., 2013; Du et al., 2018; Ezrahi et al., 2019). However, the oral bioavailability of hydrophobic drugs and nutrients is usually very low (Du et al., 2018; Ezrahi et al., 2019; Sze et al., 2019). It is of great significance to design and produce universal oral delivery systems of hydrophobic drugs and nutrients. Nanoemulsions produced from food protein and polysaccharide complexes are safe oral delivery systems of lipophilic drugs and nutrients (Evans et al., 2013; Albano et al., 2019), and can be easily scaled up for production (Singh et al., 2017). Amphipathic proteins which contain hydrophilic and hydrophobic amino acid residues in their primary structures are widely used as emulsifiers (Bouyer et al., 2012). In the process of high energy emulsification, such as ultrasound and high-pressure homogenization, amphipathic protein molecules expose their hydrophobic residues and adsorb at oil–water interface to lower the surface tension (Galazka et al., 2000; Tabibiazar et al., 2015). By means of heat treatment, the emulsions produced from globular proteins, such as BSA (bovine serum albumin) and soybean protein, form crosslinked protein film

at oil–water interface due to the denaturation and gelation of the proteins (Yin et al., 2012; Wang et al., 2016). Hydrophobic drug/nutrient can be effectively encapsulated and protected in the oil droplets (Bouyer et al., 2012, 2013; Wang, Gao, et al., 2016). Hydrophilic polysaccharide chains conjugated to the protein are located on the oil droplet surface that increase the hydrophilicity, steric repulsion and therefore the stability of the droplets in aqueous phase (Dickinson & Semenova, 1992; Dickinson, 2008). Previously, we produced curcumin-loaded BSA–dextran conjugate emulsion with crosslinked BSA interfacial film and dextran surface (Wang et al., 2016). The emulsion had long-term physical and chemical stability, and greatly increased the oral bioavailability of curcumin in mice. However, the evaluation of the therapeutic efficacy of the encapsulated drug in protein and polysaccharide complex emulsion was seldom reported, which blocks the application of the emulsion in drug delivery field.

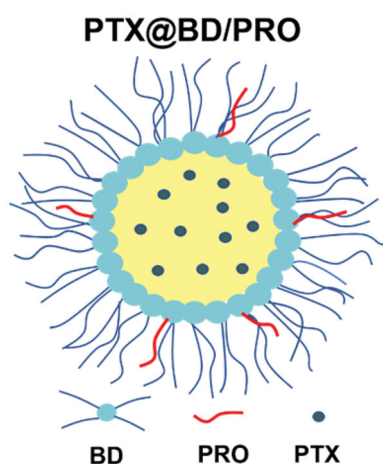
Protamine (PRO), a cationic peptide (He et al., 2014), is able to bind with negatively charged macromolecules, such as hyaluronic acid (Wang et al., 2015), carrageenan (Dul et al., 2015), heparin (Thu et al., 2012), albumin (Lochmann et al., 2005) and nucleic acid (Sköld et al., 2015), forming

CONTACT Ping Yao  yaoping@fudan.edu.cn  State Key Laboratory of Molecular Engineering of Polymers, Collaborative Innovation Center of Polymers and Polymer Composite Materials, Department of Macromolecular Science, Fudan University, Shanghai, China

 Supplemental data for this article can be accessed [here](#).

© 2020 The Author(s). Published by Informa UK Limited, trading as Taylor & Francis Group.

This is an Open Access article distributed under the terms of the Creative Commons Attribution-NonCommercial License (<http://creativecommons.org/licenses/by-nc/4.0/>), which permits unrestricted non-commercial use, distribution, and reproduction in any medium, provided the original work is properly cited.



Scheme 1. Illustration of the structure of PTX@BD/PRO emulsion droplet.

electrostatic complexes. PRO is an effective and nontoxic cell-penetrating peptide, which promotes the absorption of the bound or assembled molecules and nanoparticles in intestines (Beloqui et al., 2014; Thwala et al., 2016). For example, He et al. (2013) prepared insulin-PRO conjugate which significantly improved the pharmacological bioavailability of insulin in rats. Zhang et al. (2018) used polyethylene glycol-poly(lactic-co-glycolic acid) and PRO to fabricate exenatide-Zn²⁺ complex-loaded nanoparticles which had significant hypoglycemic effect and great improvement in oral bioavailability of exenatide. Beloqui et al. (2014) found that dextran-PRO coating greatly increased the permeability of the lipophilic drug-loaded nanoparticles in mimetic mucus and enterocyte monolayers.

Herein, we introduced PRO into BSA-dextran conjugate (BD) emulsion to increase the absorption in intestines and thus increase the oral bioavailability as well as therapeutic efficacy of the encapsulated hydrophobic drug. BD was produced by a nontoxic Maillard reaction (Qi et al., 2013; Wang et al., 2016), which links the reducing end carbonyl group of dextran to the amino group of BSA. BD is negatively charged in pH 6 solution, and therefore can bind with positively charged PRO, forming electrostatic complex BD/PRO. We used BD/PRO complex as the emulsifier to produce emulsion @BD/PRO whose structure is illustrated in Scheme 1, and used @BD/PRO to encapsulate hydrophobic antineoplastic drug paclitaxel (PTX) and fluorescent probe DiR (1,1'-dioctadecyl-3,3,3',3'-tetramethyl indotricarbocyanine iodide). The anti-tumor efficacy of orally administrated PTX-loaded @BD/PRO emulsion (PTX@BD/PRO) was evaluated and compared with the efficacy of commercial PTX injection. The systemic toxicity of PTX@BD/PRO after consecutive oral administration in mice was evaluated. In addition, BD emulsion (@BD) without PRO as well as PTX-loaded BD emulsion (PTX@BD) were produced and studied parallelly for comparison.

2. Experimental

2.1. Materials

PRO (from salmon, BC grade), dextran (10 kDa) and BSA (grade V, 99%) were obtained from Sangon Biotech Co., Ltd.

(Shanghai, China). PTX was obtained from Jiangsu Yew Pharmaceutical Co., Ltd. (Jiangsu, China). Commercial PTX injection was from Hainan Chuntch Pharmaceutical Co., Ltd. (Hainan, China). MCT (medium chain triglyceride) was purchased from Avic (Tieling) Pharmaceutical Co., Ltd. (Liaoning, China). FITC (fluorescein isothiocyanate) was obtained from Tokyo Chemical Industry Co., Ltd. (Tokyo, Japan). DiR was purchased from RuiTaibio Co., Ltd. (Beijing, China). Sodium carboxymethyl cellulose (CMC-Na) was purchased from Sigma-Aldrich (Shanghai) Co. (Shanghai, China). All other chemical reagents were purchased from Sinopharm Chemical Reagent Co., Ltd. (Shanghai, China).

2.2. Preparation of BD

BD was prepared by Maillard reaction as reported previously (Qi et al., 2013; Wang et al., 2016). Briefly, BSA and dextran were dissolved together in deionized water with a feed-molar ratio of BSA to dextran 1:6 (weight ratio of BSA to dextran 1:0.9); the mixed solution was adjusted to pH 8.0 and then lyophilized. The lyophilized powder reacted at 60 °C and 79% relative humidity for 48 h. After the reaction, about 4.4 dextran chains were conjugated to one BSA molecule on average. The produced BD was directly used without purification. For the BD solution mentioned below, the BSA concentration was used to denote the BD concentration.

2.3. Preparation of @BD/PRO and @BD emulsions

PRO and BD were added in deionized water together with 0.5 mg/mL PRO and 10 mg/mL BSA. After dissolution, the pH of the solution was adjusted to 6.0 using 1 M HCl and then the solution was stirred for 3 h to obtain BD/PRO complex solution. MCT with 20% volume fraction was added in the complex solution. The mixture was emulsified to produce oil-in-water emulsion @BD/PRO using a homogenizer (FJ200-S, Shanghai Specimen Model Co., Shanghai, China) at 10,000 rpm for 1 min followed by a high-pressure homogenizer (AH100D, ATS Engineering Inc., Shanghai, China) at 800 bar for 4 min. After a 1 h heating of the emulsion at 90 °C, the produced @BD/PRO was adjusted to pH 2.0, 5.0, 6.0 and 7.0, and then stored at 2–6 °C to investigate the stability. In addition, @BD, the emulsion without PRO, was produced using the same emulsification method.

2.4. Preparation of PTX and DiR-loaded emulsions

For the preparation of PTX@BD/PRO emulsion, PTX was dissolved in an oil phase containing 10% ethanol and 90% MCT (volume fraction) at 5 mg/mL PTX concentration, in which ethanol was acted as a cosolvent and cosurfactant; the BD/PRO complex aqueous solution, emulsification and heating conditions were the same as described in 2.3 section. DiR@BD/PRO emulsion was prepared in the same manner except that the heating was performed in the dark. For comparison, PTX@BD and DiR@BD emulsions without PRO were produced using the same BD, PTX or DiR concentrations and the same emulsification method.

2.5. Characterization

2.5.1. Complexation of PRO with BD

FITC-labeled PRO (PRO-FITC) was prepared with a feed-weight ratio of PRO to FITC 200:1 according to the literature (Yin et al., 2012; Thwala et al., 2016). BD/PRO-FITC complex solution and @BD/PRO-FITC complex emulsion were prepared using the same methods as BD/PRO and @BD/PRO. The free PRO-FITC molecules in BD/PRO-FITC solution and in @BD/PRO-FITC emulsion were separated using ultrafiltration (cutoff Mw 100 kDa). The PRO-FITC concentrations of the ultrafiltrates were analyzed on a fluorescence spectrophotometer (QM 40, Photo Technology International, Birmingham, NJ).

2.5.2. Circular dichroism (CD) spectra

The CD spectra of the PRO aqueous solution containing 0.5 mg/mL PRO were measured using a CD spectropolarimeter (Chirascan, Applied PhotoPhysics Ltd., Surrey, UK). The parameters were 0.1 cm path length, 60 nm/min scanning speed, 1 s response, 1 nm bandwidth and 1 nm data pitch.

2.5.3. ζ -Potential and dynamic light scattering (DLS)

ζ -Potential, D_h (z-average hydrodynamic diameter) and PDI (polydispersity index) were measured using a DLS instrument (Zetasizer Nano ZS90, Malvern Instruments, Malvern, UK). The ζ -potential sample was obtained after adjusting the emulsion to desired pH and then diluting the emulsion by 1000-fold with an aqueous solution having the same pH and 5 mM NaCl (Pan et al., 2007). For D_h and PDI measurement, the sample was obtained after 1000-fold dilution of the emulsions with deionized water freshly.

2.5.4. PTX loading efficiency

The free PTX molecules in 1 mL PTX@BD/PRO were extracted using 2 mL dichloromethane thrice. The dichloromethane solutions were collected, mixed and dried under reduced pressure. After being re-dissolved in acetonitrile, the extracted PTX was analyzed using HPLC (Waters e2695, Waters Corp., Milford, MA) and detected at 227 nm absorbance. The mobile phase was acetonitrile/water (70/30, v/v) containing 0.1 v% trifluoroacetic acid at a flow rate of 1.0 mL/min. Standard PTX acetonitrile solutions were analyzed at the same condition to obtain PTX work curve. The PTX loading efficiency (LE) and loading capacity (LC) in PTX@BD/PRO were calculated using the equations:

$$LE (\%) = \frac{\text{total PTX} - \text{extracted PTX}}{\text{total PTX}} \times 100\%$$

$$LC (\%) = \frac{\text{total PTX} - \text{extracted PTX}}{\text{total BSA, dextran and PRO}} \times 100\%$$

2.5.5. Transmission electron microscopy (TEM)

The diluted emulsion was deposited onto a carbon-coated copper grid. After the grid was dried, the droplets on the grid were observed on an electron microscope (FEI Tecnai

G2 TWIN, FEI Company, Hillsboro, OR). The TEM images were acquired at a magnification ratio of 14,500.

2.6. Fluorescence imaging of murine gastrointestinal tracts

All animal experiments of this study were implemented in the Experimental Animal Center, School of Pharmacy, Fudan University in full compliance with the guidelines approved by Shanghai Administration of Experimental Animals. ICR mice (male, about 20 g) were obtained from Sino-British SIPPR/BK Lab. Animal Ltd. (Shanghai, China), and were randomly divided into two groups. After an overnight fasting with free to water, each of the mice was administrated with 0.5 mL DiR@BD or DiR@BD/PRO per os. After the oral administration, the mice had free access to standard food and water; three mice in each group were sacrificed at predetermined time point, and the stomach and intestine organs were excised. The organ surfaces were washed using saline. The fluorescence images and fluorescence intensities of the organs were acquired on a small animal imaging system (In Vivo Xtreme, Bruker, Billerica, MA) as reported previously (Xu et al., 2017).

2.7. PTX oral bioavailability

ICR mice (male) were randomly divided into four treatment groups. Before administration, the mice were fasting overnight but free to water. In PTX injection group, the commercial PTX injection was intravenously injected (*i.v.*) at a PTX dose of 12 mg/kg. In the three oral groups, PTX/CMC-Na suspension prepared by dispersing PTX in 1% CMC-Na aqueous solution with 1 mg/mL PTX concentration (Hou et al., 2017), PTX@BD and PTX@BD/PRO were separately administrated by intragastric gavage (*i.g.*) at a PTX dose of 20 mg/kg. After the administration, the mice had free access to water and standard chow. At each predetermined interval, in each group, five mice were sampled from eye ground vein. About 500 μ L blood sample was put into EDTA-preprocessed microtube and centrifuged at 1810 *g* and 4 °C (TGL-16G, Shanghai Anting Scientific Instruments, Shanghai, China) for 10 min immediately. The plasma of 150 μ L was taken out and mixed with 350 μ L acetonitrile. The mixture was vortexed for 2 min and then centrifuged at 4 °C and 7260 *g* for 15 min. The supernatant of 50 μ L was loaded onto the HPLC system for PTX analysis as described above. The PTX bioavailability (BA) of the oral groups was calculated using the following equation:

$$BA (\%) = \frac{(AUC_{0-24})_{i.g.} \times \text{Dose}_{i.v.}}{(AUC_{0-24})_{i.v.} \times \text{Dose}_{i.g.}} \times 100\%$$

where AUC_{0-24} is the area under PTX plasma concentration-time curve from 0 to 24 h, and Dose is the PTX dose administrated.

2.8. Anti-tumor efficacy evaluation

Male ICR mice were inoculated with 2×10^6 murine ascites hepatoma H22 cells in right hindquarter. The inoculated mice were randomly divided into five groups and each group had 9 mice. On the day of 3, 5, 7 and 9 after the inoculation, the commercial PTX injection was intravenously injected at a PTX dose of 12 mg/kg; the commercial PTX injection, PTX@BD and PTX@BD/PRO were orally administered by intragastric gavage at a PTX dose of 30 mg/kg separately. The oral saline group was acted as the control group. On the day 10, the mice were sacrificed; the tumors were excised and weighted. TIR (tumor inhibition ratio) was calculated using the equation:

$$\text{TIR (\%)} = (1 - \text{WT}/\text{WC}) \times 100\%$$

where WT and WC are the tumor weights of the treatment and control groups, respectively. The PA (pharmacological availability) of the oral groups was calculated on the basis of TIR using the equation:

$$\text{PA (\%)} = \frac{\text{TIR}_{i.g.} \times \text{Dose}_{i.v.}}{\text{TIR}_{i.v.} \times \text{Dose}_{i.g.}} \times 100\%$$

2.9. In vivo safety evaluation after long-term administration

Male ICR mice were randomly divided into four treatment groups. In PTX injection group, the commercial PTX injection was intravenously injected at a PTX dose of 10 mg/kg. In the oral groups, PTX@BD and PTX@BD/PRO were orally administered at a PTX dose of 30 mg/kg separately, and the control group was orally administered with the same volume of saline. The administration was performed on every other day. After 13 times of the administration, the mice were sacrificed. The organs of stomach, intestine, spleen, heart, lung, liver, and kidney were excised. The hematoxylin-eosin (H&E) stained organ sections were prepared as described previously (Liu et al., 2017), and the histological images of the sections were obtained on a microscope (BX53, OLYMPUS, Tokyo, Japan).

2.10. Statistical analysis

The data were displayed as mean \pm standard deviation. Statistical analysis was carried out using the independent samples *t*-test. *p* value $< .05$ between two groups was considered significantly different.

3. Results and discussion

3.1. Properties of @BD/PRO and @BD emulsions

PRO is rich in arginine residues, its *M_w* is about 5.1 kDa and isoelectric point is 10–12 (He et al., 2014). At pH 6.0, PRO was positively charged, BSA of BD was negatively charged, and therefore PRO and BD formed electrostatic complex. We used fluorescence probe FITC-labeled PRO and ultrafiltration (cutoff *M_w* 100 kDa) to characterize the complexation of PRO

with BD. In the individual PRO-FITC solution, all the free PRO-FITC molecules passed across the ultrafiltration membrane, and the ultrafiltrate displayed a strong PRO-FITC fluorescence signal as shown in Figure 1(A). In the PRO-FITC and BD mixed solution, only 0.2% of the PRO-FITC molecules passed across the ultrafiltration membrane, indicating that 99.8% of the PRO-FITC molecules bound with BD, forming BD/PRO-FITC complex.

BD/PRO complex was used as emulsifier to produce @BD/PRO. After emulsification at pH 6.0, the produced emulsion was heat-treated at 90 °C for 1 h to cause BSA denaturation and gelation, consequently to form crosslinked oil–water interfacial film (Qi et al., 2013; Wang et al., 2016). The heat treatment did not result in the PRO degradation and conformation change, verified by Figure S1 of Supplementary material, which shows the identical CD spectra of the individual PRO aqueous solution before and after the heat treatment. Due to the complexation with BSA, the hydrophilic PRO chains might be anchored in the crosslinked oil–water interfacial film. In @BD/PRO-FITC emulsion, only 0.7% of the PRO-FITC molecules passed across the ultrafiltration membrane (Figure 1(A)), confirming that 99.3% of the PRO-FITC molecules were fixed in the interfacial film. The ζ -potential of free PRO solution was zero because the PRO was too small to be measured. Compared with @BD, @BD/PRO increased the positive charges on the droplet surface in pH 2–8 range, as shown in Figure 1(B), indicating that the other end of the fixed PRO chains stretched in the aqueous phase. The results shown in Figure 1(A,B) substantiated that PRO chains were successfully introduced into @BD/PRO by binding PRO with BD and fixing the PRO chains in the crosslinked interfacial film.

Table 1 shows that at the same emulsification condition except PRO concentration, the produced emulsions with and without PRO had different droplet sizes. The *D_h* of @BD/PRO was 302 nm, while the *D_h* of @BD was 197 nm. The fresh @BD/PRO samples prepared at pH 6.0 were adjusted to pH 2.0, 5.0 and 7.0. After 60 days of storage at 2–6 °C, all the samples were homogeneous in appearance and their droplet sizes did not change significantly (Figure 1(C)), suggesting that the @BD/PRO produced at pH 6.0 was very stable in pH 2.0–7.0 media. The @BD/PRO was also produced at pH 7.0 at which BD and PRO also carried opposite charges. The *D_h* of @BD/PRO produced at pH 7.0 was 296 nm (Figure S2 of Supplementary material), almost the same as the *D_h* of @BD/PRO produced at pH 6.0. The @BD/PRO produced at pH 7.0 also presented long-term stability after 40 days of storage at 2–6 °C in pH 2.0, 5.0 and 7.0 media. In the following sections, the emulsions produced at pH 6.0 were further studied.

3.2. Properties of PTX- or DiR-loaded @BD/PRO and @BD emulsions

We used @BD/PRO to encapsulate antineoplastic drug PTX and near infrared fluorescence probe DiR. The PTX loading efficiency and loading capacity of the emulsion was 99.7% and 6.4%, respectively (Table 1). The *D_h* and ζ -potential of PTX@BD/PRO at pH 6.0 were 288 nm and -1.6 mV, close to

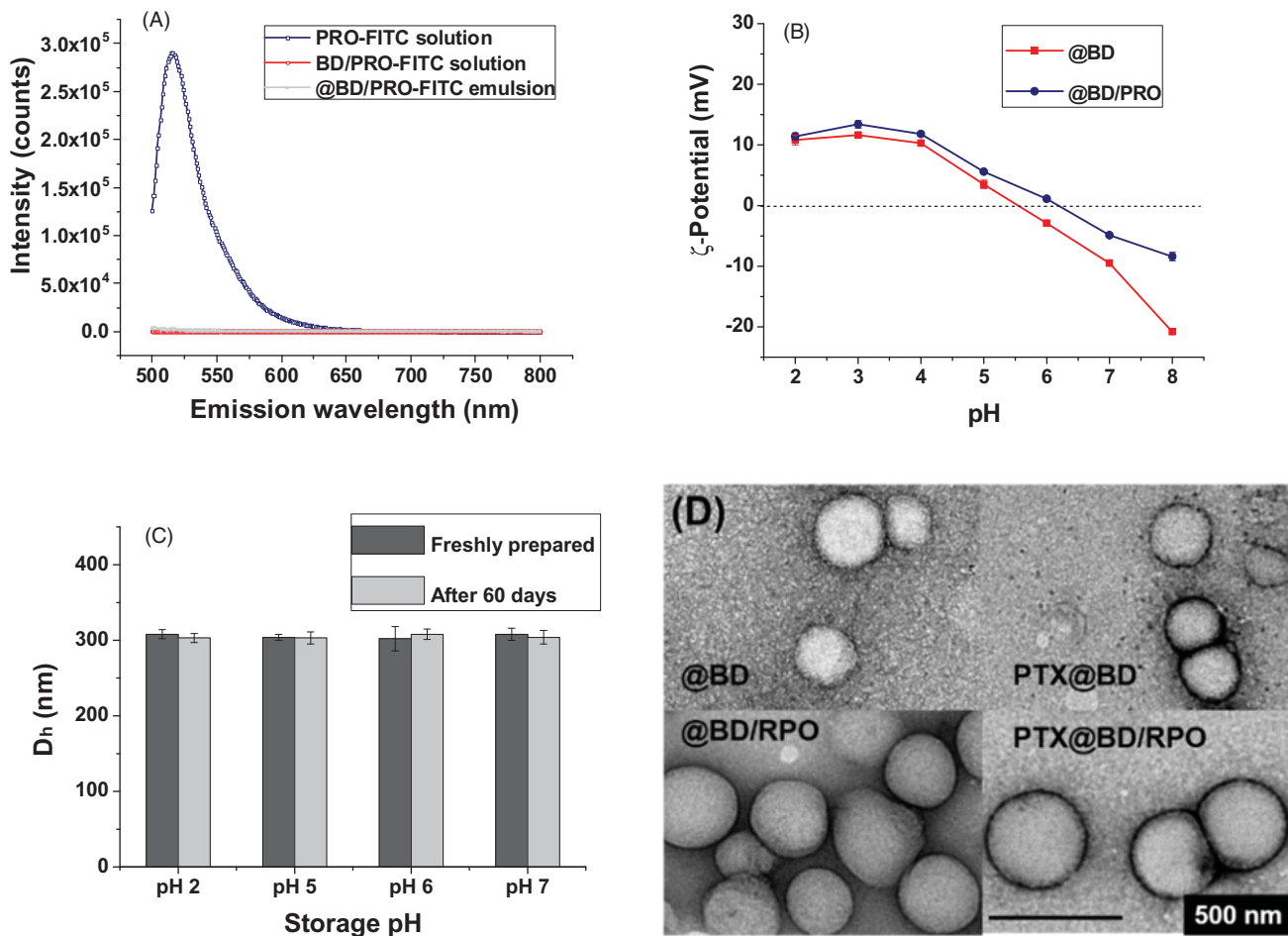


Figure 1. (A) Fluorescence intensities of the ultrafiltrates of PRO-FITC solution, BD/PRO-FITC solution and @BD/PRO-FITC emulsion; (B) ζ -potential changes of @BD and @BD/PRO emulsions as the function of pH; (C) D_h values of @BD/PRO emulsion after adjustment to pH 2.0, 5.0 and 7.0 and then storage at 2–6 °C ($n = 3$); (D) TEM images of @BD, PTX@BD, @BD/RPO and PTX@BD/RPO emulsions. The emulsions were prepared at pH 6.0.

Table 1. Properties of PTX and DiR-loaded emulsions ($n = 3$).

Sample ^a	Freshly prepared						After 120 days	
	Drug concentration (mg/mL)	Loading efficiency (%)	Loading capacity (%)	ζ -Potential (mV)	D_h (nm)	PDI	D_h (nm)	PDI
@BD	0	–	–	-3.5 ± 0.8	197 ± 10	0.07 ± 0.05	187 ± 3	0.04 ± 0.01
PTX@BD	1.00	99.6 ± 0.2	6.6 ± 0.1	-3.2 ± 0.4	193 ± 5	0.04 ± 0.02	189 ± 3	0.10 ± 0.02
DiR@BD	0.08	–	–	-3.9 ± 0.5	191 ± 8	0.06 ± 0.04	183 ± 9	0.08 ± 0.06
@BD/PRO	0	–	–	-1.7 ± 0.5	302 ± 16	0.04 ± 0.03	312 ± 10	0.17 ± 0.04
PTX@BD/PRO	1.00	99.7 ± 0.1	6.4 ± 0.1	-1.6 ± 0.7	288 ± 5	0.04 ± 0.03	289 ± 3	0.11 ± 0.06
DiR@BD/PRO	0.08	–	–	-1.4 ± 0.4	277 ± 6	0.04 ± 0.03	295 ± 6	0.06 ± 0.06

^aThe emulsions were produced at pH 6.0; the BSA concentration was 8 mg/mL and dextran concentration was 7.2 mg/mL in all the emulsions; the PRO concentration was 0.4 mg/mL in the emulsions containing PRO.

the D_h and ζ -potential of @BD/PRO, respectively. DiR@BD/PRO had similar D_h and ζ -potential as PTX@BD/PRO. For comparison, PTX@BD and DiR@BD without PRO were produced. The emulsions with and without PRO had almost the same loading efficiencies, but the D_h values of PTX@BD and DiR@BD were 95 and 86 nm smaller than those of PTX@BD/PRO and DiR@BD/PRO, respectively. The TEM images in Figure 1(D) display the spherical morphology of @BD, PTX@BD, @BD/RPO and PTX@BD/RPO droplets. All the droplets in the images had integrated interfacial film and coalescence was not obvious. Some droplets were close to each other which might occur during the drying process because

the droplets in the solutions were well dispersible as indicated by their narrow PDI values of 0.04–0.07 (Table 1). All the emulsions with and without PRO were stored at 2–6 °C in pH 6.0 medium. After 120 days of storage, all the emulsions were homogeneous in appearance, their D_h values did not change significantly, indicating that all the emulsions had long-term physical stability. It is reasonable that the emulsions had good stability because the droplets were protected and stabilized by the crosslinked interfacial film and were dispersed in aqueous solutions by the conjugated dextran chains as reported previously (Qi et al., 2013; Wang et al., 2016).

3.3. In vitro digestion of PTX@BD and PTX@BD/PRO

It was reported that polysaccharide could delay the enzymatic degradation of protein-based nanoparticles in gastrointestinal tract (Chang et al., 2017; Alavi et al., 2018). The sequential digestions of PTX@BD and PTX@BD/PRO in simulated gastric fluid (SGF) and simulated intestinal fluid (SIF) were investigated as reported previously (Xu et al., 2017). As shown in Figure S3 of Supplementary material, the emulsions remained homogenous in appearance after 2 h digestion in SGF, and only 1% of the PTX was extractable by dichloromethane, implying that the emulsions are not digestible or the digestion is very slow in stomach. In the followed digestion in SIF, each of the mixtures became two layers. The lower layer was transparent, the upper layer was cloudy with oil and chyme, and most of the PTX was extractable by dichloromethane, suggesting that the emulsions can be digested in intestine.

3.4. Fluorescence imaging of murine gastrointestinal tracts

After oral administration of DiR@BD and DiR@BD/PRO separately in mice, the *ex vivo* fluorescence images of the murine gastrointestinal tracts were acquired. The two groups presented similar fluorescence distributions in gastrointestinal tracts as shown in Figure 2(A,B) and Figure S4 of Supplementary material. In both groups, the fluorescence intensities in the stomachs decreased gradually. In the intestines, the jejunums and ileums exhibited relatively higher fluorescence intensities, suggesting that the emulsions and/or their digestive products stayed in jejunums and ileums for longer time. According to the literature (Thirawong et al., 2008), the retention in jejunum and ileum would be beneficial to the absorption of the delivered drug.

3.5. Oral PTX bioavailability of PTX@BD and PTX@BD/PRO

Figure 2(C,D) and Table 2 respectively show the PTX plasma concentration–time curves and corresponding PTX pharmacokinetic parameters. In PTX injection group, commercial PTX injection was injected *via* caudal vein at 12 mg/kg PTX dose, the C_{max} (maximum PTX plasma concentration) was 11280 ng/mL, and the AUC_{0-24} was 7660 h·ng/mL. In oral PTX/CMC-Na suspension group at the PTX dose of 20 mg/kg, the BA was 8.2% relative to PTX injection group, which was similar to the result reported in the reference (Sparreboom et al., 1997). In PTX@BD and PTX@BD/PRO oral groups, their relative BA values were 24.4% and 34.6%, which were 3.0 and 4.2-fold of the BA value of the oral PTX/CMC-Na suspension group, respectively. Possibly, two factors resulted in the higher BA values of the emulsions. One factor is that dextran is a lymphatic absorption enhancer (Jonsson, 1977; Muranishi et al., 1997). For example, Soudry-Kochavi et al. (2015) reported crosslinked BSA and dextran nanoparticles for oral delivery of exenatide, which improved the relative BA of exenatide to about 77% due to the enhanced lymphatic uptake

in enterocytes by the dextran on the coating wall of the nanoparticles. The other factor is that the oil in the emulsion droplets can be released, hydrolyzed, assembled into mixed micelles and chylomicrons, absorbed in intestines and transported into systemic circulation *via* portal vein and lymphatic system (Tso & Balint, 1986; Kotta et al., 2012; Kim et al., 2018), which would increase the absorption and transportation of the solubilized and delivered lipophilic drug (Porter et al., 2007; Kotta et al., 2012; Carrière, 2016). Because both dextran and oil droplets could promote the absorption of the encapsulated drug and also the lymphatic transport could reduce hepatic first-pass effect, it was reasonable that both PTX@BD and PTX@BD/PRO emulsions greatly enhanced the PTX plasma concentrations compared with PTX/CMC-Na suspension. Furthermore, the BA of PTX@BD/PRO was 42% higher than that of PTX@BD, displaying that PRO had a substantial contribution to the PTX absorption. Because PRO can promote the absorption of the bound or assembled molecules and nanoparticles in intestines (He et al., 2013; Belouqui et al., 2014; Thwala et al., 2016; Zhang et al., 2018), the PRO fixed on the interfacial film and stretched in the aqueous phase increased the absorption of PTX@BD/PRO in intestine and therefore increased the PTX plasma concentration.

As shown in Figure 2(C,D), after a single intravenous injection, the PTX plasma concentration of the commercial PTX injection group reached to 11280 ng/mL at 0.25 h post-injection. After reaching to the C_{max} , the PTX plasma concentration dropped rapidly. The concentration was 36 ng/mL at 12 h post-administration, much lower than the defined therapeutic concentration of 85.3 ng/mL (Yang et al., 2004; Joshi et al., 2013). In contrast, the three oral groups kept their PTX plasma concentrations steadily during 0–24 h. The PTX plasma concentrations of PTX@BD and PTX@BD/PRO oral groups at 24 h post-administration were 112 and 178 ng/mL, respectively, significantly higher than the PTX therapeutic concentration of 85.3 ng/mL. These data indicated that PTX@BD and PTX@BD/PRO would prolong the action time of PTX.

3.6. Tumor inhibition efficacy of PTX@BD and PTX@BD/PRO

The anti-tumor efficacies were evaluated in H22 tumor-bearing mice. As shown in Table 3 and Figure 3, the TIR of the commercial PTX injection group was 44% and the TIR of PTX@BD/PRO oral group was 43%. This result indicated that PTX@BD/PRO oral group had the same tumor inhibition efficacy as commercial PTX injection group. The PA of PTX@BD/PRO oral group reached to 39% relative to PTX injection group, while the PA of PTX@BD oral group was 23%. The H22 tumor inhibition efficacy of PTX@BD/PRO was 70% higher than the efficacy of PTX@BD. The average body weight of PTX@BD/RPO oral group was larger than the weight of the commercial PTX injection group, as shown in Figure S5 of Supplementary material, although the oral PTX dose was 2.5-fold of the injected PTX dose. These results indicated that at the same tumor inhibition efficacy, the

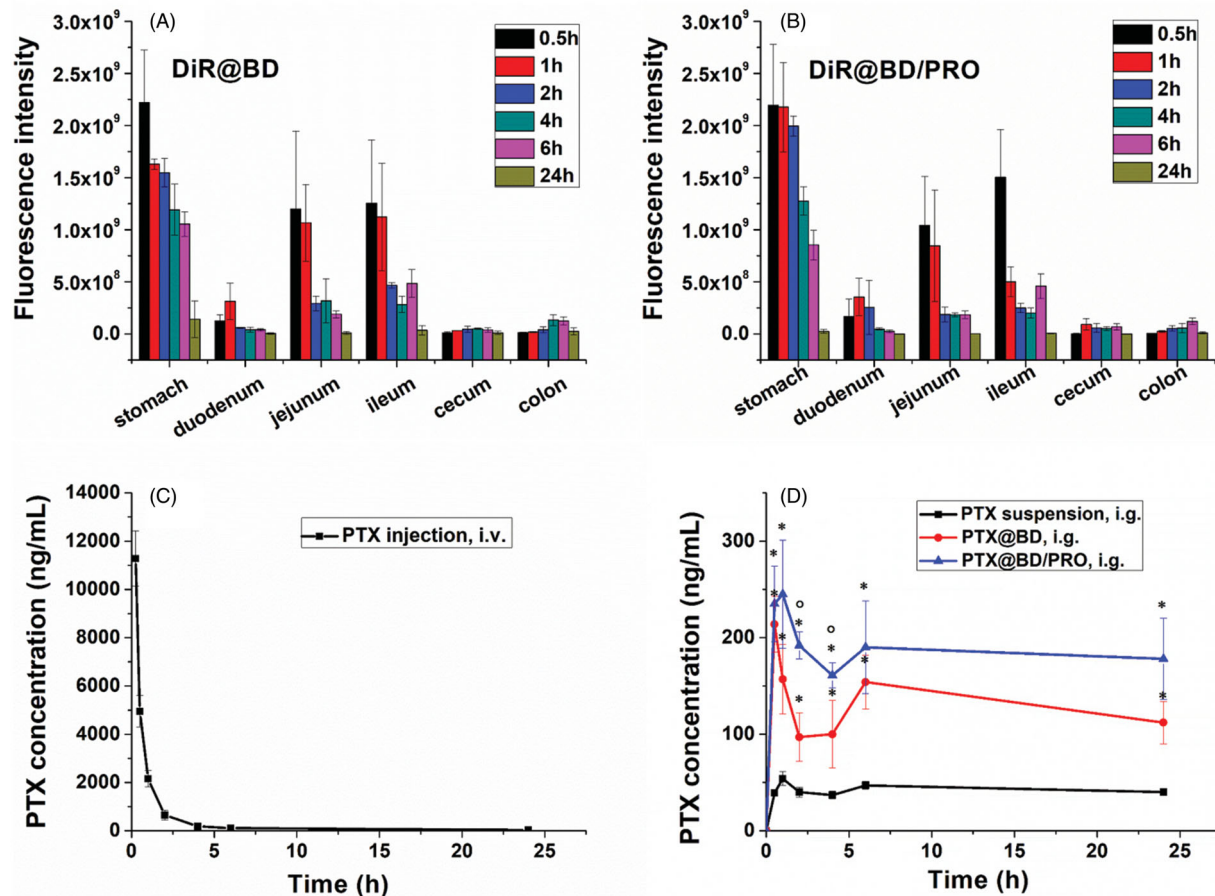


Figure 2. Fluorescence intensities of the murine gastrointestinal tracts excised at 0.5, 1, 2, 4, 6 and 24 h after the oral administration of (A) DiR@BD and (B) DiR@BD/PRO separately ($n = 3$). PTX plasma concentrations of the mice after (C) intravenous injection of commercial PTX injection at a PTX dose of 12 mg/kg, and (D) oral administration of PTX/CMC-Na suspension, PTX@BD and PTX@BD/PRO emulsions separately at a PTX dose of 20 mg/kg ($n = 5$); * $p < .01$ compared with the suspension group; $^{\circ}p < .05$ compared with the PTX@BD group.

Table 2. Pharmacokinetic parameters of PTX ($n = 5$).

Group	Treatment manner	PTX dose (mg/kg)	Tmax (h)	Cmax (ng/mL)	AUC ₀₋₂₄ (h·ng/mL)	BA (%)
PTX injection	i.v.	12	0.25	11280	7660	100
PTX/CMC-Na suspension	i.g.	20	1	54	1042	8.2
PTX@BD	i.g.	20	0.5	214	3118	24.4
PTX@BD/PRO	i.g.	20	1	245	4413	34.6

Table 3. Tumor inhibition effects of the H22 tumor-bearing mice after various treatments ($n = 9$).

Group	Treatment manner	PTX dose (mg/kg)	Mice number (beginning/end)	Average tumor weight (g)	TIR (%)	PA (%)
Saline	i.g.	0	9/9	0.68 ± 0.20	–	–
PTX injection	i.v.	12	9/9	0.38 ± 0.10 ^{a,b}	44	100
PTX oral	i.g.	30	9/9	0.63 ± 0.18	7	6
PTX@BD	i.g.	30	9/9	0.51 ± 0.20	25	23
PTX@BD/PRO	i.g.	30	9/9	0.39 ± 0.11 ^{a,b}	43	39

^a $p < .01$ compared with saline group.

^b $p < .01$ compared with PTX oral group.

orally administrated PTX@BD/RPO was more biocompatible than the intravenously injected commercial PTX injection.

3.7. In vivo safety after long-term administration

To further evaluate the biocompatibility of the emulsions and safety of the treatments, histological analysis of the organs was carried out after 13 times of consecutive administration in healthy mice. In PTX injection group, vacuolar

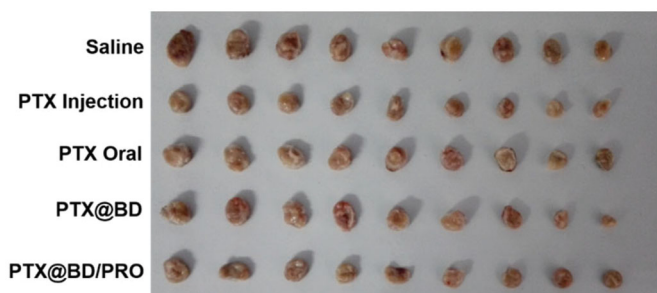


Figure 3. Photo of the tumors after various treatments ($n = 9$).

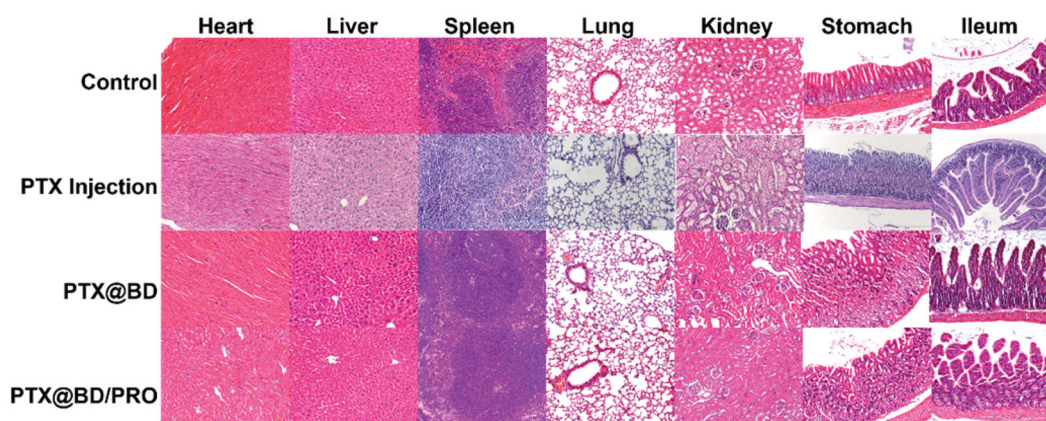


Figure 4. Representative H&E stained histological images of the murine organs excised after 13 times of the consecutive intravenous injection of commercial PTX injection at a PTX dose of 10 mg/kg and consecutive oral administration of PTX@BD and PTX@BD/PRO emulsions separately at a PTX dose of 30 mg/kg.

degeneration appeared in liver cells and edema occurred in renal tubular epithelial cells as shown in Figure 4, verifying that the commercial PTX injection had liver and kidney toxicity after long-term consecutive intravenous injection. Although the oral PTX dose was three-fold of the injected PTX dose, PTX@BD and PTX@BD/PRO oral groups did not show any abnormality in the main organs including stomach and ileum after the consecutive oral administration, testifying that the orally administered PTX@BD and PTX@BD/PRO were biocompatible and safe after long-term oral administration. This study displayed that PTX@BD and PTX@BD/PRO reduced the toxicity and enhanced the tumor inhibition efficacy of PTX, which were similar to the functions of orally administered selenium nanoparticles with polysaccharide–protein complex coating reported by Zhang et al. (2019) recently.

4. Conclusions

In this study, the electrostatic complex of PRO and BD was used as the emulsifier to produce emulsion for encapsulation and oral delivery of hydrophobic drug PTX. The BSA molecules were crosslinked by a heat treatment and the PRO chains were simultaneously anchored in the oil–water interface. BD emulsion without PRO was produced for comparison. The emulsions had 99% PTX loading efficiency, 6.4% loading capacity and long-term stability. The bioavailability and H22 tumor inhibition efficacy of PTX@BD/PRO were 40% and 70% higher than those of PTX@BD, respectively, after oral administration in the mice. Compared with the intravenously injected commercial PTX injection, orally administered PTX@BD/PRO had the same tumor inhibition efficacy, and PTX@BD/PRO was biocompatible and safe after long-term oral administration. For the first time, this study displays that orally administered drug-loaded protein and polysaccharide complex emulsion can achieve the same therapeutic efficacy as the commercial injection. Besides PTX and DiR, @BD/PRO can encapsulate other oil-soluble drugs and nutrients. @BD/PRO is a universal carrier for encapsulation and oral delivery of hydrophobic drugs and nutrients, and is promising for practical application.

Disclosure statement

The authors report no conflict of interest.

Funding

This study was financially supported by National Natural Science Foundation of China [No. 21474018 and 21274026].

References

- Alavi F, Emam-Djomeh Z, Yarmand MS, et al. (2018). Cold gelation of curcumin loaded whey protein aggregates mixed with k-carrageenan: impact of gel microstructure on the gastrointestinal fate of curcumin. *Food Hydrocolloids* 85:267–80.
- Albano KM, Cavallieri ÂLF, Nicoletti VR. (2019). Electrostatic interaction between proteins and polysaccharides: physicochemical aspects and applications in emulsion stabilization. *Food Rev Int* 35:54–89.
- Beloqui A, Angeles Solinis M, Des Rieux A, et al. (2014). Dextran-protamine coated nanostructured lipid carriers as mucus-penetrating nanoparticles for lipophilic drugs. *Int J Pharm* 468:105–11.
- Bouyer E, Mekhloufi G, Huang N, et al. (2013). β -Lactoglobulin, gum arabic, and xanthan gum for emulsifying sweet almond oil: formulation and stabilization mechanisms of pharmaceutical emulsions. *Colloids Surf, A* 433:77–87.
- Bouyer E, Mekhloufi G, Rosilio V, et al. (2012). Proteins, polysaccharides, and their complexes used as stabilizers for emulsions: alternatives to synthetic surfactants in the pharmaceutical field? *Int J Pharm* 436: 359–78.
- Carrière F. (2016). Impact of gastrointestinal lipolysis on oral lipid-based formulations and bioavailability of lipophilic drugs. *Biochimie* 125: 297–305.
- Chang C, Wang T, Hu Q, et al. (2017). Caseinate-zein-polysaccharide complex nanoparticles as potential oral delivery vehicles for curcumin: effect of polysaccharide type and chemical cross-linking. *Food Hydrocolloids* 72:254–62.
- Dickinson E. (2008). Interfacial structure and stability of food emulsions as affected by protein-polysaccharide interactions. *Soft Matter* 4: 932–42.
- Dickinson E, Semenova MG. (1992). Emulsifying properties of covalent protein dextran hybrids. *Colloids Surf* 64:299–310.
- Du X, Khan AR, Fu M, et al. (2018). Current development in the formulations of non-injection administration of paclitaxel. *Int J Pharm* 542: 242–52.
- Dul M, Paluch KJ, Kelly H, et al. (2015). Self-assembled carrageenan/protamine polyelectrolyte nanoplexes—Investigation of critical parameters governing their formation and characteristics. *Carbohydr Polym* 123: 339–49.

- Evans M, Ratcliffe I, Williams PA. (2013). Emulsion stabilisation using polysaccharide-protein complexes. *Curr Opin Colloid Interface Sci* 18: 272–82.
- Ezrahi S, Aserin A, Garti N. (2019). Basic principles of drug delivery systems—the case of paclitaxel. *Adv Colloid Interface Sci* 263:95–130.
- Galazka VB, Dickinson E, Ledward DA. (2000). Influence of high pressure processing on protein solutions and emulsions. *Curr Opin Colloid Interface Sci* 5:182–7.
- He H, Sheng J, David AE, et al. (2013). The use of low molecular weight protamine chemical chimera to enhance monomeric insulin intestinal absorption. *Biomaterials* 34:7733–43.
- He H, Ye J, Liu E, et al. (2014). Low molecular weight protamine (LMWP): a nontoxic protamine substitute and an effective cell-penetrating peptide. *J Control Release* 193:63–73.
- Hou J, Sun E, Zhang Z, et al. (2017). Improved oral absorption and anti-lung cancer activity of paclitaxel-loaded mixed micelles. *Drug Deliv* 24:261–9.
- Jonsson KTTL. (1977). Cellular distribution of orally and intramuscularly administered iron dextran in newborn piglets. *Can J Comp Med* 41: 318–25.
- Joshi N, Saha R, Shanmugam T, et al. (2013). Carboxymethyl-chitosan-tethered lipid vesicles: hybrid nanoblock for oral delivery of paclitaxel. *Biomacromolecules* 14:2272–82.
- Kim KS, Suzuki K, Cho H, et al. (2018). Oral nanoparticles exhibit specific high-efficiency intestinal uptake and lymphatic transport. *ACS Nano* 12:8893–900.
- Kotta S, Khan AW, Pramod K, et al. (2012). Exploring oral nanoemulsions for bioavailability enhancement of poorly water-soluble drugs. *Expert Opin Drug Deliv* 9:585–98.
- Liu Z, Xu G, Wang C, et al. (2017). Shear-responsive injectable supramolecular hydrogel releasing doxorubicin loaded micelles with pH-sensitivity for local tumor chemotherapy. *Int J Pharm* 530:53–62.
- Lochmann D, Weyermann J, Georgens C, et al. (2005). Albumin-protamine-oligonucleotide nanoparticles as a new antisense delivery system. Part 1: physicochemical characterization. *Eur J Pharm Biopharm* 59: 419–29.
- Muranishi S, Fujita T, Murakami M, et al. (1997). Potential for lymphatic targeting of peptides. *J Contr Rel* 46:157–64.
- Pan X, Yu S, Yao P, et al. (2007). Self-assembly of beta-casein and lysozyme. *J Colloid Interface Sci* 316:405–12.
- Porter CJH, Trevaskis NL, Charman WN. (2007). Lipids and lipid-based formulations: optimizing the oral delivery of lipophilic drugs. *Nat Rev Drug Discov* 6:231–48.
- Qi J, Huang C, He F, et al. (2013). Heat-treated emulsions with cross-linking bovine serum albumin interfacial films and different dextran surfaces: effect of paclitaxel delivery. *J Pharm Sci* 102:1307–17.
- Singh Y, Meher JG, Raval K, et al. (2017). Nanoemulsion: concepts, development and applications in drug delivery. *J Contr Rel* 252:28–49.
- Sköld AE, Van Beek JJ, Sittig SP, et al. (2015). Protamine-stabilized RNA as an ex vivo stimulant of primary human dendritic cell subsets. *Cancer Immunol Immunother* 64:1461–73.
- Soudry-Kochavi L, Naraykin N, Nassar T, et al. (2015). Improved oral absorption of exenatide using an original nanoencapsulation and microencapsulation approach. *J Control Release* 217:202–10.
- Sparreboom A, Van Asperen J, Mayer U, et al. (1997). Limited oral bioavailability and active epithelial excretion of paclitaxel (Taxol) caused by P-glycoprotein in the intestine. *Proc Natl Acad Sci U S A* 94: 2031–5.
- Sze LP, Li HY, Lai KLA, et al. (2019). Oral delivery of paclitaxel by polymeric micelles: a comparison of different block length on uptake, permeability and oral bioavailability. *Colloids Surf B Biointerfaces* 184: 110554.
- Tabibiazar M, Davaran S, Hashemi M, et al. (2015). Design and fabrication of a food-grade albumin-stabilized nanoemulsion. *Food Hydrocolloids* 44:220–8.
- Thanki K, Gangwal RP, Sangamwar AT, et al. (2013). Oral delivery of anti-cancer drugs: challenges and opportunities. *J Control Release* 170: 15–40.
- Thirawong N, Thongborisute J, Takeuchi H, et al. (2008). Improved intestinal absorption of calcitonin by mucoadhesive delivery of novel pectin-liposome nanocomplexes. *J Control Release* 125:236–45.
- Thu MS, Bryant LH, Coppola T, et al. (2012). Self-assembling nanocomplexes by combining ferumoxytol, heparin and protamine for cell tracking by magnetic resonance imaging. *Nat Med* 18:463–7.
- Thwala LN, Beloqui A, Csaba NS, et al. (2016). The interaction of protamine nanocapsules with the intestinal epithelium: a mechanistic approach. *J Control Release* 243:109–20.
- Tso P, Balint JA. (1986). Formation and transport of chylomicrons by enterocytes to the lymphatics. *Am J Physiol Gastrointest Liver Physiol* 250:G715–G26.
- Wang C, Liu Z, Xu G, et al. (2016). BSA-dextran emulsion for protection and oral delivery of curcumin. *Food Hydrocoll* 61:11–9.
- Wang L, Gao Y, Li J, et al. (2016). Effect of resveratrol or ascorbic acid on the stability of α -tocopherol in O/W emulsions stabilized by whey protein isolate: simultaneous encapsulation of the vitamin and the protective antioxidant. *Food Chem* 196:466–74.
- Wang S, Cao M, Deng X, et al. (2015). Degradable hyaluronic acid/protamine sulfate interpolyelectrolyte complexes as miRNA-delivery nanocapsules for triple-negative breast cancer therapy. *Adv Healthc Mater* 4:281–90.
- Xu G, Wang C, Yao P. (2017). Stable emulsion produced from casein and soy polysaccharide compacted complex for protection and oral delivery of curcumin. *Food Hydrocoll* 71:108–17.
- Yang SC, Gursoy RN, Lambert G, et al. (2004). Enhanced oral absorption of paclitaxel in a novel self-microemulsifying drug delivery system with or without concomitant use of P-glycoprotein inhibitors. *Pharm Res* 21:261–70.
- Yin B, Deng W, Xu K, et al. (2012). Stable nano-sized emulsions produced from soy protein and soy polysaccharide complexes. *J Colloid Interface Sci* 380:51–9.
- Zhang L, Shi Y, Song Y, et al. (2018). The use of low molecular weight protamine to enhance oral absorption of exenatide. *Int J Pharm* 547: 265–73.
- Zhang Z, Du Y, Liu T, et al. (2019). Systematic acute and subchronic toxicity evaluation of polysaccharide-protein complex-functionalized selenium nanoparticles with anticancer potency. *Biomater Sci* 7:5112–23.